Diameter-defined Strahler system and connectivity matrix of the pulmonary arterial tree

Z. L. JIANG, G. S. KASSAB, AND Y. C. FUNG
Institute for Biomedical Engineering, University of California, San Diego, La Jolla, California 92093–0412

Jiang, Z. L., G. S. Kassab, and Y. C. Fung. Diameter-defined Strahler system and connectivity matrix of the pulmonary arterial tree. *J. Appl. Physiol.* 76(2): 882–892, 1994.—For modeling of a vascular tree for hemodynamic analysis, the well-known Weibel, Horsfield, and Strahler systems have three shortcomings: vessels of the same order are all treated as in parallel, despite the fact that some are connected in series; histograms of the diameters of vessels in the successive orders have wide overlaps; and the "small-twigs-on-large-trunks" phenomenon is not given a quantitative expression. To improve the accuracy of the hemodynamic circuit model, we made a distinction between vessel segments and vessel elements: a segment is a vessel between two successive nodes of bifurcation; an element is a union of a group of segments of the same order that are connected in series. In an equivalent circuit, all elements of the same order are considered as arranged in parallel. Then, we follow the ordering method of Horsfield and Strahler, with introduction of an additional rule for the assignment of order numbers. If D_n and SD_n denote the mean and standard deviation of the diameters of vessels of *order n*, then our rule divides the gap between $D_n - SD_n$ and $D_{n-1} + SD_{n-1}$ evenly between *orders n* and $n - 1$. Finally, we introduced a connectivity matrix with a component in the *m*th row and the *n*th column that is the average number of vessels of *order m* that grow out of the vessels of *order n*. This method was applied to the rat. We found that the rat pulmonary arterial tree has 11 orders of vessels and that the geometry is fractal within these orders. The ratios of diameters, lengths, and numbers of elements in successive orders are 1.58, 1.60, and 2.76, respectively. The connectivity matrix reveals interesting features beyond the fractal concept. New features are found in the variation of the total cross-sectional area of elements with order numbers.

anatomy; pulmonary artery; branching ratio; vessel segment; vessel elements; fractal; network; lung; rat

MORPHOMETRY IS USUALLY DONE for a purpose. Weibel (25, 26) did it to estimate the pulmonary gas diffusion capacity. Cumming et al. (1), Sobin et al. (22, 23), Singhal et al. (20), Horsfield and Gordon (9, 12), and Yen et al. (30, 31) did it for the analysis of the pulmonary circulation. Skalak and Schmid-Schönbein (21) did it for blood flow in the skeletal muscle. Jiang and He (14, 15) and Kassab et al. (16) did it for the coronary blood flow. This study is aimed at the modeling of the pulmonary vasculature for hemodynamic analysis (2–4, 7, 29, 32, 33). A statement of the objective is important, because the objective dictates the selection of the parameters for measurement and the method of organization of the data. With regard to the parameter selection, we note that the most important formula for blood flow is that of Poiseuille, which states that the flow rate ($\dot{Q}$) of a Newtonian fluid of coefficient of viscosity μ in a circular cylindrical tube of lumen diameter D and length L subjected to an inlet pressure P_i and exit pressure P_e is (2)

$$\dot{Q} = \frac{\pi D^4 (P_i - P_e)}{128 \mu L} \quad (1)$$

D appears in the fourth power; a 10% error in D leads to a 46.4% error in $\dot{Q}$, whereas a 10% error in any other parameter, such as P_i, P_e, μ, and L, leads to only a 10% error in $\dot{Q}$. Hence, among all parameters on the right-hand side of *Eq. 1*, D is the most demanding for accuracy. *Equation 1* is valid if the entry and exit velocity profile is parabolic and if the pressure is uniformly distributed in all cross sections. If these conditions are not exactly fulfilled or if the flow is turbulent or oscillatory, then the right-hand side of *Eq. 1* will have to be multiplied by a numerical factor that depends on the exact boundary conditions and the Reynolds and Womersley numbers, which in turn depend on D. Thus D dominates in all cases.

For hemodynamics, the data should be organized to produce a reliable analogue circuit. For the pulmonary vasculature, we have to describe how the vessels of different sizes are connected into a circuit. For the lung, Fung and Sobin (5) showed that the capillaries are connected like a sheet but the arteries and veins are connected like a tree. Weibel (25) modeled the arterial tree as a bifurcation system; other authors (9, 20, 31) modeled the arterial tree as a Strahler system, which is a modification of a model of rivers proposed by Horton (13) for geography. In the basic Strahler (24) and Horsfield (9, 12) systems, every vessel between two nodes of bifurcation is recognized as a segment. Segments with the smallest diameters are called vessels of *order 1*. When two vessels of *order 1* meet, the confluent is called a vessel of *order 2*. Two vessels of *order 2* meet to yield a vessel of *order 3*, and so on. However, if a vessel of *order 1* meets a vessel of *order 2*, the confluent remains at *order 2*. A vessel of *order 3* meeting another vessel of *order 1* or *2* remains *order 3*, and so on. This is illustrated in Fig. 1, except for a subtree at the *lower right-hand corner* in *A*, which represents a case often encountered in which two vessels of *order 2* meet but the confluent is no larger than the original. In this case, Strahler would have called the confluent vessel *order 3*, but the diameter-defined system to be explained later would continue to refer to the confluent vessel as *order 2* (see Fig. 1 and text surrounding *Eq. 3*, *A* and *B*). The Strahler system is a major improvement over the bifurcation system (25), because it takes into account the asymmetric branching pattern.

A defect of the Horsfield method (9, 12) is that no distinction is made between series and parallel segments of the same order in the vascular trees. For example, in Fig. 1, the *order 4* segments at the *top* in *A* are counted as three segments, despite the fact that they are connected in series and function as one resistor. Horsfield (11) rec-

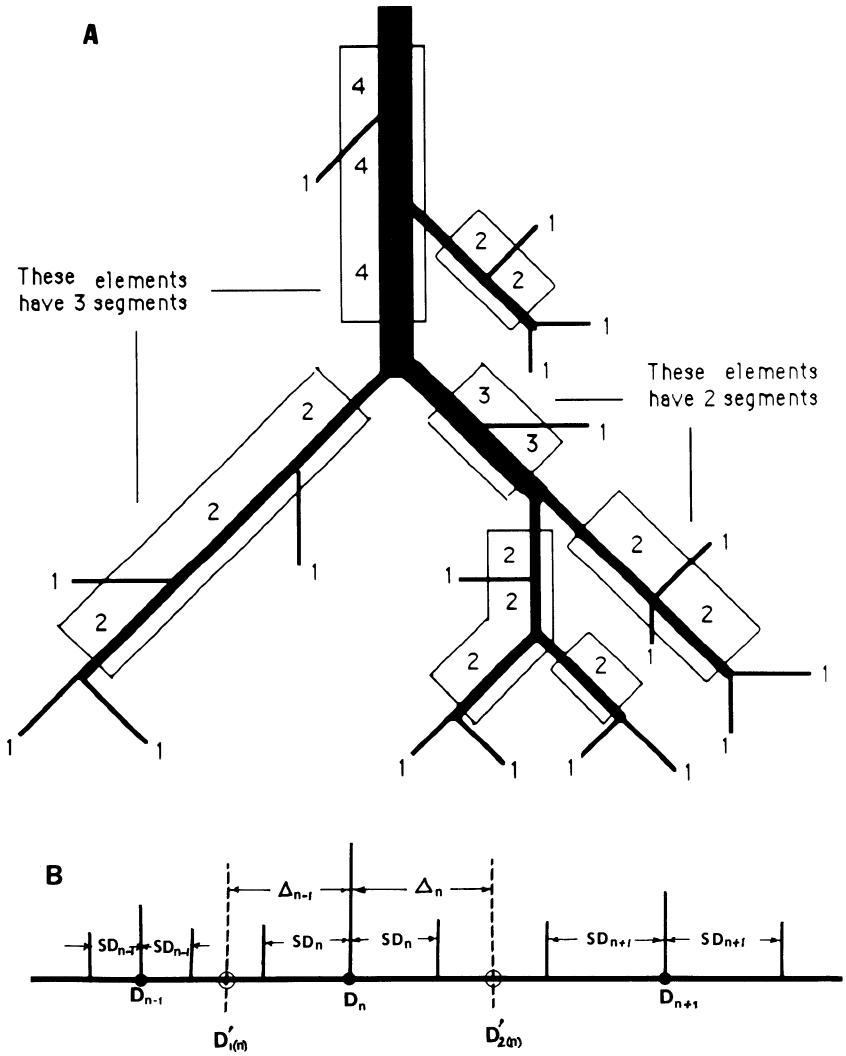

FIG. 1. *A*: pattern of scheme of our diameter-defined Strahler system. Vessel order numbers are determined by their connection and diameters. Each vessel between 2 successive points of bifurcation is defined as a segment. Segments of the same order connected in series are defined as an element. Smallest segments and elements are of *order 1*. When 2 elements meet, order number is that of larger element (assumed to be $n - 1$) increased by 1 (to *order n*) if diameter of confluent element is larger than a certain value specified by *Eq. 3A*. Elements of *orders 4* (from elements of *orders 3* and *2*) and *3* (from 2 *order 2* elements) meet this criterion. On the other hand, if diameter of confluent element is smaller than value specified by *Eq. 3B*, then order number of confluent element is not increased, as shown in lower branch on *right-hand side*, where 2 *order 2* vessels meet to generate another *order 2* element, when diameters are tested by *Eq. 3B* with $n = 2$. *B*: plot of diameters of successive orders of arteries (D_{n-1}, D_n, and D_{n+1}) on a straight line. Gaps between $D_{n-1} + SD_{n-1}$ and $D_n - SD_n$ and between $D_n + SD_n$ and $D_{n+1} - SD_{n+1}$ are split in the middle by dashed lines. We define order numbers by means of these dashed lines, which are represented by *Eq. 3*.

ognized the fact that all vessel segments of a given order are not in parallel in the sense of an analogue electric circuit and suggested that a better representation could be obtained by the original Strahler method (24), which does not change order number of a tapering vessel, no matter how long and how much smaller its diameter becomes as long as it intersects only smaller branches. Horsfield (11) called this a "Strahler method stage 2" but did not give any data. As a remedy to this defect, we combine each group of segments of a given order connected in series and call it an element. Thus, in Fig. 1*A*, the three *order 4* segments represent one element. The three *order 2* segments on the branch on the *left-hand side* is another element. The total number of vessel elements of a given order is, of course, smaller than the total number of vessel segments of that order. Thus, in Fig. 1, there are 5 *order 2* elements but 11 *order 2* segments. The lower right branch is related to the diameter-defined concept to be explained later. In an analogue electric circuit of the vasculature, elements are connected according to the connectivity matrix. Another defect of the Weibel, Horsfield, and Strahler systems is that there are large overlaps of the statistical frequency functions of the diameters in the successive orders of vessels. An example for the rat's lung analyzed by the Horsfield method is shown in Fig. 2, in which the histograms representing the numbers of the pulmonary arterial segments and elements of *orders 6–8* are plotted against the diameters. The diameters of the segments and elements of *order 6* are 90–300 μm, those of *order 7* are 200–500 μm, and those of *order 8* are 300–700 μm. The large overlaps of these histograms are caused by the large number of branches in a large tree. The effect is discussed later.

The third problem concerns the small branches projecting from larger trunks. All blood vessels of *order n* do not arise from vessels of *order* $n + 1$: they may arise also from vessels of *orders* $n + 2$, $n + 3$, ... In general, a vessel of *order m* is connected to a larger vessel of *order n* at one end ($n > m$) and a smaller vessel of *order* $m - 1$ at the other end. The pressure in this vessel varies from the entry pressure, which is the pressure in the vessel of *order n*, (P_n), to the exit pressure, which is the pressure in the vessel of *order* $m - 1$, (P_{m-1}). P_n and P_{m-1} are spatially variable: each varies from a maximum at the entry to a minimum at the exit. With P_n and P_{m-1} so defined, the flow in the vessel of *order m* issuing from a vessel of *order n* is, according to *Eq. 1*

$$\dot{Q}_{mn} = \frac{\pi D_m^4 (P_n - P_{m-1})}{128 \mu L_m} \quad (2)$$

where D_m and L_m are diameter and length, respectively, of the vessel of *order m*. Hence, $\dot{Q}_{mn}$ can be computed only

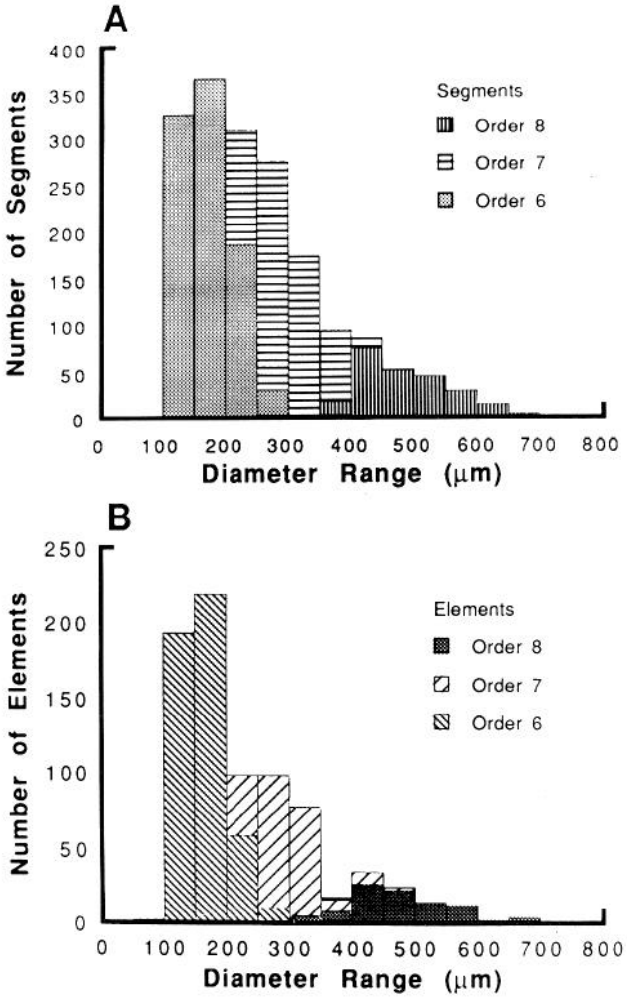

FIG. 2. Histograms of diameters of successive orders of pulmonary arteries of rat when branching order numbers were determined according to conventional method of Strahler (24) and Horsfield (9, 11). Note extensive overlaps of histograms of successive orders.

if the vessel's origin in *order n* and exit into a vessel of *order m* − 1 are known. Thus the connection between vessels of *orders m* and *n* is important from the point of view of blood vessel circuit modeling. This aspect has not been dealt with so far.

To remedy these difficulties, we introduce a segment-to-element ratio, a diameter-defined Strahler system, and a connectivity matrix: the first to account for the series-parallel feature, the second to eliminate the overlap of the histograms of the diameters of the vessel elements in the successive orders, and the third to describe the way in which the elements of different orders in the tree are connected. The details are explained below and are illustrated by the pulmonary arterial trees of the rats.

As a matter of record, the concept of the diameter-defined Strahler system was used in our laboratory by Fung and Yen for the pulmonary arteries of the dog in 1987 (unpublished observations) and was developed by Kassab et al. (16) in their study of the coronary blood vessels of the pig. The connectivity matrix was first used for the pig coronary arteries by Kassab et al.

METHODS

Eleven Sprague-Dawley rats weighing 410–450 g (429.9 ± 12.4 g) were used: five were used for polymer casts and six for histological slides.

Pulmonary Arterial Tree Casts

Each rat was anesthetized with pentobarbital sodium (50 mg/kg ip). The trachea was exposed and cannulated, and the lung was ventilated. The blood was anticoagulated with heparin (10 mg/kg iv), and then a lethal dose of pentobarbital sodium was given intravenously. The chest was opened by a midline thoracotomy, and the lungs and heart were exposed. The airway pressure was then held constant at 10 cmH_2O (1 kPa) above the pleural pressure, which was atmospheric. Through a cannula inserted into the main pulmonary artery, the pulmonary vessels were perfused with a low-viscosity (25-cP) silicone elastomer (Microfil CP-101, Flow Tech, Boulder, CO), which was freshly catalyzed with an accelerator consisting of 4% stannous octoate and 2% ethyl silicate and mixed with 0.25% Cab-O-Sil (Eastman Kodak), an inert powder with particles large enough to form clusters that obstructed the free flow of fluid through the pulmonary capillaries. The silicone fluid was drained from a cannula inserted in the left atrium that was maintained at zero pressure. After the lung was perfused at 30 cmH_2O for 5 min, the perfusing pressure was lowered to 20 cmH_2O and held constant. Approximately 2 h were needed for the silicone elastomer to harden. The animal was then kept in a refrigerator overnight or longer to increase the strength of the silicone rubber. The dependence of the fluidity and hardening process of the silicone polymer on the concentration of the catalysts has been investigated in detail by Fung et al. (6); our protocol yields the arterial casts. Then the lungs and heart were removed and suspended in a 10% KOH solution for 2 or 3 days to corrode away the veins and other tissue. A typical cast is shown in Fig. 3. Sobin et al. (22, 23) showed that, in an equivalent polymer (GE compound 88017, not available commercially), the volumetric expansion in solidification was <1%.

Histological Slides

The branching patterns of small blood vessels were measured from the histological sections of the left lungs of six rats. The animals were prepared in the manner described above. Each lung was perfused first with a clear catalyzed silicone elastomer and then with the same elastomer mixed with 0.25% Cab-O-Sil. After the perfusing pressure was lowered to 20 cmH_2O and held constant, the left atrial cannula was closed to stop the flow. After the elastomer hardened, the lung was fixed

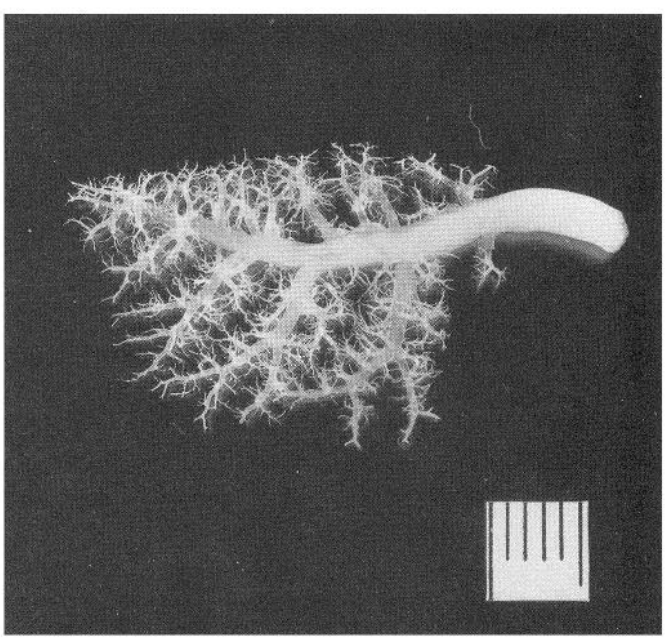

FIG. 3. Polymer cast of arterial tree of rat left lung. Length scale, 5 mm.

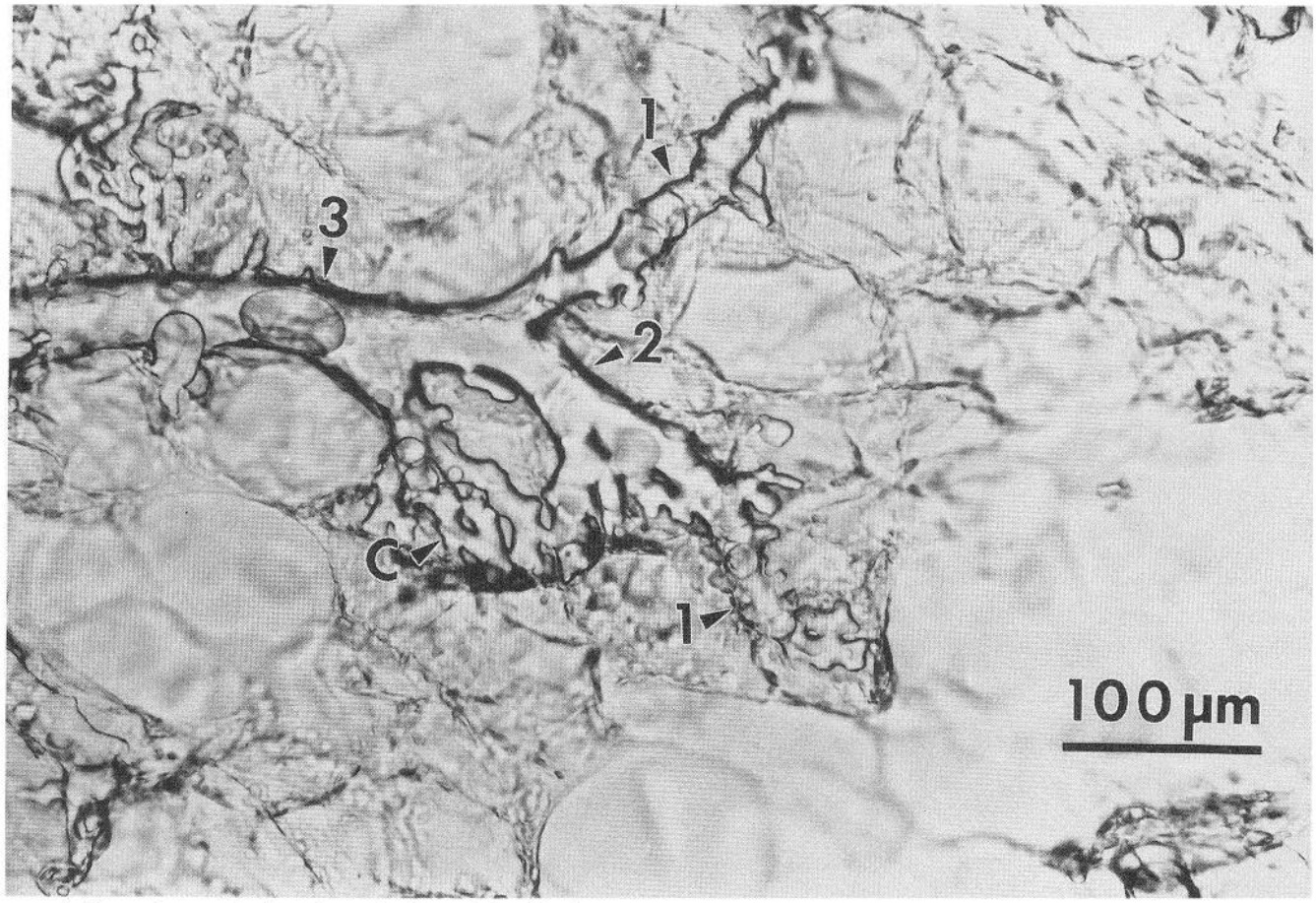

FIG. 4. Photomicrograph of rat lung showing relationship between capillary bed and several orders of arteries. Arteries were perfused with catalyzed silicone elastomer containing 0.25% Cab-O-Sil. Section thickness, 40 μm. C, capillaries; 1, arteries of *order 1*; 2, arteries of *order 2*; 3, artery of *order 3*.

by instillation of a 2.5% glutaraldehyde solution buffered by phosphate to pH 7.4 into the trachea at 10 cmH_2O pressure. Then the lung was embedded in a 20% gelatin solution, hardened in a 10% formaldehyde solution, and sectioned at 40-, 60-, and 80-μm thicknesses and mounted in glycerol without staining.

Measurements of the Tree Casts

An image-processing system was built to measure the sizes of the pulmonary vessels. The system consists of an IBM-AT computer with the software DT2851 by Data Translation (Marlborough, MA) and a dissection microscope (Olympus), a video camera (COHU), and a video monitor (Sony Trinitron). The Petri dish containing the polymer casts or the histological slides are put on a Lucite plate that can be rotated about the optical path (z) and about a horizontal axis (y). The vascular trees were observed through the dissection microscope at ×20 magnification. The vascular images were "grabbed" by the computer, digitized, and analyzed. Several measurements of the lumen diameter were made along each vessel segment and averaged to obtain the mean diameter of the segment. The length of a vessel segment was obtained by measuring the distance between bifurcation points along the center line of the segment after the segment was rotated first about z to parallel with x and then about y until the segmental length was maximal.

From one of the five left pulmonary arterial tree casts, a complete set of data of the lumen diameters and lengths of all vessel segments of the tree was obtained. This was done step by step as follows. The main trunk of the left pulmonary artery was sketched, and its segments were measured. The subtrees arising from the main trunk were cut down and labeled further, cut, sketched, and measured. This process was continued until every segment, including the smallest twigs, was measured. For the other four casts, the same process was followed for all vessel segments with diameters >250 μm. Then five subtrees of each cast were chosen randomly and measured by the method described above for all their segments, including the smallest twigs; the other subtrees were pruned and cast away.

Measurements of Histological Specimens and Definition of Vessels of Order 1

The histological specimens were viewed with an inverted microscope at ×400 magnification. The images were displayed on a video monitor through a video camera. The dimensions of all segments with diameters <70 μm were measured.

The smallest noncapillary blood vessels were assigned to *order 1*. In the histological slides, it was not difficult to identify these *order 1* vessels, because Cab-O-Sil effectively prevented filling of the capillary blood vessels (Fig. 4).

Description of Branching Pattern

Diameter-defined Strahler system. We use the Strahler system that calls capillary vessels *order 0*, and larger arteries have higher order numbers. The original rules of ordering according to Strahler (24) and Horsfield (9, 10) are as follows: *1*) when two vessels of the same order meet, the confluent offspring's order number is increased by 1, and *2*) when a vessel of *order n* meets another vessel of order <n, then the order number of the offspring remains n. These rules sound simple, but they have practical difficulties. For example, in *case 1*, the two meeting vessels of the same order number can have very different diame-

TABLE 1. *Connectivity matrix for hypothetical tree illustrated in Fig. 1*

	1	*2*	*3*	*4*
1	0	3.2	1.0	1.0
2	0	0.2	2.0	2.0
3	0	0	0	1.0
4	0	0	0	0

ters, so an actual situation may look like a large trunk meeting a twig. In *case 2*, the diameter of the vessel of smaller order may not be smaller than the diameter of the higher-order vessel or the offspring may, in fact, have a considerably larger diameter; yet the order number is not allowed to increase. To resolve these difficulties, we replace these original rules with a new rule: when an artery of *order n* meets another vessel of *order* $\leq n$, the order number of the confluent offspring is increased to $(n + 1)$ if, and only if, its diameter is greater than those of the two parents by an amount that is determined by a scheme shown in Fig. 1*B*. Here D_n is the mean diameter of the vessels of *order n* and SD_n is their standard deviation. On a straight line, the diameters D_{n-1}, D_n, and D_{n+1} are plotted and one standard deviation, SD_{n-1}, SD_n, and SD_{n+1}, was marked on either side of D_{n-1}, D_n, and D_{n+1}. There is a gap between the markers $D_n + SD_n$ and $D_{n+1} - SD_{n+1}$. Take the midline between these markers and label its distance to D_n by Δn. Then, when a vessel of *order n* meets another vessel of *order* $< n$, the order number of their confluent offspring is increased by 1 (to $n + 1$) if, and only if, its diameter exceeds $D_n + \Delta n$. Otherwise the order number of the offspring remains n. Now, the width of the gap to the right of D_n is $[(D_{n+1} - SD_{n+1}) - (D_n + SD_n)]$. The coordinate of the midway point of the gap is

$$D_n + SD_n + \tfrac{1}{2}(D_{n+1} - SD_{n+1} - D_n - SD_n) = \tfrac{1}{2}(D_{n+1} + D_n - SD_{n+1} + SD_n) = D_n + \Delta_n$$

This may be written as $D'_{2(n)}$. Similarly we can find the coordinate of the midway point of the gap to the left of D_n and denote it by $D'_{1(n)}$. Thus we see that the rule for deciding the order number may be stated in a different but equivalent way as follows: a vessel is said to be of *order n* if its diameter is within the following limits

$$D'_{1(n)} = [(D_{n-1} + SD_{n-1}) + (D_n - SD_n)]/2 \quad (3A)$$

$$D'_{2(n)} = [(D_n + SD_n) + (D_{n+1} - SD_{n+1})]/2 \quad (3B)$$

where $D'_{1(n)}$ is the lower limit and $D'_{2(n)}$ is the upper limit. To implement this rule, an iteration procedure is used. First, each vessel is assigned an order number according to the original scheme of Strahler (24) and Horsfield (9, 12), and the mean values and standard deviations of the diameters, D_n and SD_n, of vessels of *order n* are computed for $n = 1, 2, 3, \ldots$. Then we use *Eq. 3* to revise the order number of the vessels. After revision, the new values of D_n and SD_n are computed for $n = 1, 2, 3, \ldots$, and the process is repeated until convergence is obtained. We consider the process converged when the changes between successive iterations become <1%. Two or three cycles are generally enough to reach convergence.

TABLE 2. *Segmental data of rat left pulmonary arterial tree*

Order No.	Diam of Segments,* μm	No. of Segments†	Length of Segments,* mm	No. of Segments Measured
11	1,638±193	8±1	2.26±1.73	40
10	938±136	13±2	1.11±0.65	63
9	613±73	28±3	0.69±0.36	140
8	404±44	49±3	0.63±0.30	246
7	262±36	146±4	0.47±0.21	657
6	156±24	346±9	0.39±0.18	664
5	89.9±13	777±11	0.29±0.12	1,355
4	60.5±5.1	1,540±18	0.23±0.09	1,012
3	43.7±4.0	4,098±61	0.18±0.08	628
2	31.1±5.3	12,789±453	0.11±0.07	703
1	13.3±3.2	63,961±1,452	0.04±0.02	571

Pleural pressure = atmospheric pressure; airway pressure = 10 cmH_2O; pressure in left atrium = 0 cmH_2O. * Means ± SD; † means ± SE.

Combining segments into elements and measuring diameter and length of elements. A blood vessel segment is one between two successive nodes of bifurcation. Segmental length is measured along the center line of the vessel. An element is formed by segments of the same order that are connected in series (Fig. 1). The lengths of elements are recorded. The diameter of an element is computed as the average of the diameters of the segments that makes up the element.

Order numbers of elements of an arterial tree. After the diameters of the elements are determined, the order numbers of the elements are checked again according to the rules set down in *Diameter-defined Strahler system*, and *Eq. 3* is applied to the elements to obtain a tree of elements.

Connectivity matrix of tree. The connectivity matrix is a square array of numbers. The number in the mth row and the nth column is denoted by $\mathbf{C}_{mn}$, which represents the average ratio of the number of elements of *order m* springing from elements of *order n* divided by the total number of elements in *order n*. The meaning of the matrix can be illustrated in a hypothetical branching tree shown in Fig. 1, in which 16 vessels of *order 1* are connected to 5 elements of *order 2*, yielding an average of 16/5 = 3.2 *order 1* vessels connected to each element of *order 2*. Also, in Fig. 1, there is no vessel coming from another vessel of *order 1*, whereas there is one *order 1* vessel coming from an element of *order 3* and another one coming from an element of *order 4*. Hence, we write, in this case, $C_{11} = 0$, $C_{12} = 3.2$, $C_{13} = 1$, and $C_{14} = 1$. These values are entered into the first row of Table 1. Furthermore there are five elements of *order 2*, one of which is connected to another element of *order 2*, yielding an average of $C_{22} = 1/5 = 0.2$, whereas two are connected to an element of *order 3*, yielding $C_{23} = 2$, and two are connected to an element of *order 4*, yielding $C_{24} = 2$. Thus, in the second row of Table 1, the entries are 0, 0.2, 2.0, and 2.0. Similarly, the entries of the third and fourth rows of Table 1 are obvious. Generalizing to a tree with k orders, we obtain a $k \times k$ matrix. Only $\mathbf{C}_{mn}$ with $n \geq m$ is meaningful in the Strahler system. We fill the matrix for entries with $n < m$ with zeroes. In final results concerning large trees (see Table 4), the entries $\mathbf{C}_{mn}$ are means ± SE. The standard error is equal to the standard deviation divided by the square root of the number of observations.

Counting total number of elements in each order. The connectivity matrix can be used to compute the total number of elements in each order. For the tree of Fig. 1, the total number of parallel elements in each order, N_m, can be calculated from $\mathbf{C}_{mn}$ as follows

$$N_4 = 1$$

$$N_3 = C_{34}N_4 + C_{33}N_3 = 1 \times 1 + 0 \times 1 = 1$$

$$N_2 = C_{24}N_4 + C_{23}N_3 + C_{22}N_2 = 2 \times 1 + 2 \times 1 + 0.2 \times 5 = 5$$

$$N_1 = C_{14}N_4 + C_{13}N_3 + C_{12}N_2 + C_{11}N_1 = 1 \times 1 + 1 \times 1 + 3.2 \times 5 + 0 \times 18 = 18$$

In general

$$N_m = \sum_{n=m}^{k} \mathbf{C}_{mn}N_n \quad (4)$$

where N_n is the number of elements of *order n* and the summation is for $n = m$ to the highest order of the tree, k.

TABLE 3. *Elemental data of rat left pulmonary arterial tree*

Order No.	Diam of Elements		No. of Elements†	Length of Elements		NS/NE*	No. of Elements Measured
	μm*	*DR*		mm*	*LR*		
11	1,639±83	1.76	1	18.11±1.81	6.86	8.00±1.23	5
10	929±97	1.54	5	2.64±1.94	1.52	2.52±1.62	23
9	602±57	1.44	11±1	1.74±1.35	1.31	2.54±1.88	54
8	417±40	1.57	23±1	1.33±0.69	1.07	2.14±1.20	117
7	266±30	1.75	56±2	1.24±0.60	1.72	2.60±1.33	280
6	152±25	1.73	183±18	0.72±0.42	1.80	1.89±1.04	435
5	88.1±11	1.43	555±38	0.40±0.23	1.48	1.40±0.66	1,032
4	61.5±4.6	1.39	1,351±71	0.27±0.13	1.35	1.14±0.37	741
3	44.4±4.9	1.40	3,794±319	0.20±0.09	1.33	1.08±0.45	782
2	31.7±4.9	2.38	7,993±852	0.15±0.07	3.00	1.60±1.14	404
1	13.3±2.8		52,001±4,378	0.05±0.03		1.23±0.56	402

Pleural pressure = atmospheric pressure; airway pressure = 10 cmH_2O; pressure in left atrium = 0 cmH_2O. *DR* (diam ratio) = D_{n+1}/D_n; *LR* (length ratio) = L_{n+1}/L_n; NS/NE, ratio of no. of segments to no. of elements. Total no. of elements in *orders 7–11* is avg of 5 casts; total no. in *orders 1–6* is calculated from connectivity matrix. * Means ± SD; † means ± SE.

When *Eq. 4* is applied to a tree, some of the branches of which were pruned, we must keep track of the order number of the elements that are cut and the total number of the cuts that are made at each order. Each cut deletes a subtree. In counting the total number of elements, we must add back the number of lost branches. In this case, we may write, with N'_n as the number of elements of *order n* pruned

$$N_m = \sum_{n=m}^{k} \mathbf{C}_{mn}(N_n + N'_n) \tag{5}$$

The standard error of the total number of elements in each order can be calculated according to the rule of propagation of errors. Taking differentials of *Eq. 5* and noting that N'_n are known to the gardener for each pruning procedure, we have

$$\Delta N_m = \sum_{n=m}^{k} \Delta\mathbf{C}_{mn}(N_n + N'_n) + \mathbf{C}_{mn}\Delta N_n \tag{6}$$

The differentials ΔN_m and $\Delta\mathbf{C}_{mn}$ may be interpreted as standard errors.

Meshing of Data From Histological Slides With Those From Polymer Casts

The histological slides provided the data for the first four orders of the arterial elements. Taking the mean and standard deviations of the vessels of *orders 3* and *4* in the histological slides, we assigned order numbers to the vessels in the tree casts, first according to the Strahler rules and then iterated according to the diameter-defined rule. Our assumption is that the data from the slides and casts are equally valid. This is plausible because the casts and slides were made of the same polymer under the same protocol.

RESULTS

Our experimental results from the left pulmonary arterial trees of 11 rats are presented in Tables 2–4. The data in Table 2 are for segments; those in Tables 3 and 4 are for elements. Table 2 presents the diameters, lengths, and total numbers of segments of all orders. The ratios of the number of segments of each order to the number of elements of the same order are listed in Table 3. The total numbers of elements of *orders 7–11* were counted directly from the five casts, whereas those of *orders 1–6* were calculated from the connectivity matrix shown Table 4 according to *Eqs. 5* and *6*.

The ratios of diameters and lengths of elements in successive orders are listed in Table 3 as *DR* (the diameter ratio) and *LR* (the length ratio).

The total number of orders of the arterial tree for the left lung of the rat was found to be 11. A very short segment of the main pulmonary artery where the left and right pulmonary arteries join may be considered as an element of *order 12* for the whole lung.

In Fig. 5, the diameters and lengths of the elements in millimeters are plotted in logarithmic scale against the order number. Straight regression lines were determined by the least-squares method. If y represents the logarithm of diameter and x represents the order number, then the regression line is $y = -1.0072 + 0.1987x$ (r =

TABLE 4. *Connectivity matrix of elements of rat left pulmonary arterial tree*

	1	*2*	*3*	*4*	*5*	*6*	*7*	*8*	*9*	*10*	*11*
1	0.19±0.03	4.06±0.15	2.48±0.35	1.36±0.40	0	0	0	0	0	0	0
2	0	0.12±0.03	1.55±0.09	0.93±0.22	0	0	0	0	0	0	0
3	0	0	0.17±0.07	2.26±0.05	0.31±0.03	0.05±0.01	0.11±0.05	0.13±0.07	0	0	0
4	0	0	0	0.05±0.02	2.00±0.04	0.70±0.06	0.62±0.10	0.43±0.12	0.39±0.29	0	0
5	0	0	0	0	0.18±0.02	1.92±0.07	1.56±0.13	0.85±0.16	0.83±0.26	0.50±0.34	0
6	0	0	0	0	0	0.18±0.02	2.05±0.13	1.15±0.15	1.00±0.29	0.67±0.33	0
7	0	0	0	0	0	0	0.05±0.02	1.55±0.14	1.06±0.21	0.67±0.33	0
8	0	0	0	0	0	0	0	0.08±0.04	1.67±0.23	0.83±0.40	6
9	0	0	0	0	0	0	0	0	0.06±0.06	1.67±0.49	4
10	0	0	0	0	0	0	0	0	0	0.17±0.17	2
11	0	0	0	0	0	0	0	0	0	0	0

Values are means ± SE. A component $\mathbf{C}_{mn}$ in *row m* and *column n* is ratio of total no. of elements of *order m* springing from elements of *order n* divided by total no. of elements in *order n*.

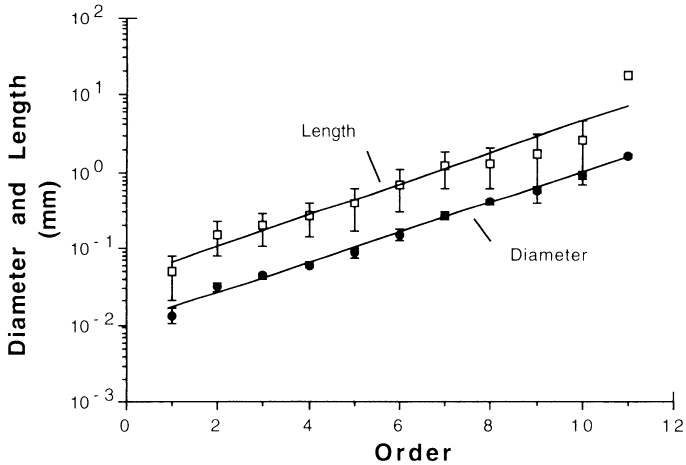

FIG. 5. Correlation of order number with average diameter and length of elements in each order of arteries of rat left lung.

0.9970). The slope is 0.1987. Its antilog gives an average diameter ratio of 1.58 between successive orders. Similarly, if y represents the logarithm of the length of the elements in a given order x, then $y = -1.3890 + 0.2043x$ ($r = 0.9670$) describes the least-squares fit, and the average length ratio between the successive orders is 1.60. The relationship between the logarithms of the number of elements (y) in the left lung of a rat and the order number (x) is shown in Fig. 6, with a regression line of $y = 4.9373 - 0.4413x$ ($r = 0.9970$), which yields an average element numbers ratio of 2.76 between successive orders.

Figures 2 and 7 show six typical histograms of random samples of the populations of diameter data of segments and elements of *orders 6–8* determined by the Strahler and diameter-defined methods, respectively. They exhibit rough approximations of the shape of the probability frequency distributions of the diameters of segments and elements of different orders. A set of raw data for these histograms of elements is shown in Tables 5 and 6. For brevity of presentation, we use ~10-μm intervals for <100-μm arteries and 50-μm intervals for >100-μm arteries. Table 5 shows the number of elements of each order in successive intervals of diameters when the branching order numbers were determined according to the conventional method of Strahler and Horsfield. The values in Table 5 are those in random samples of a size that is equal to the sum total of each column. The sample size is

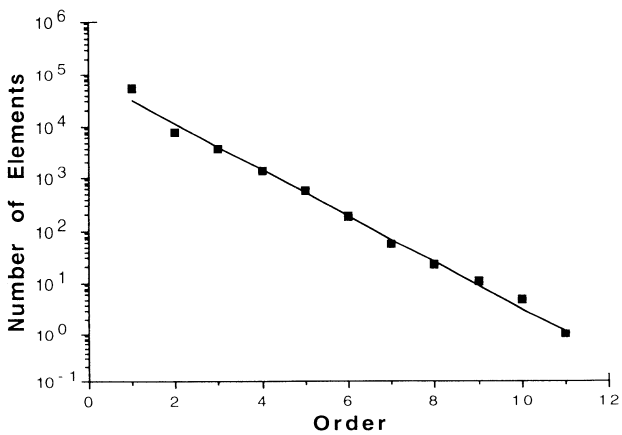

FIG. 6. Relationship between order number and average number of elements in each order. SE bars in y direction are too small to be seen.

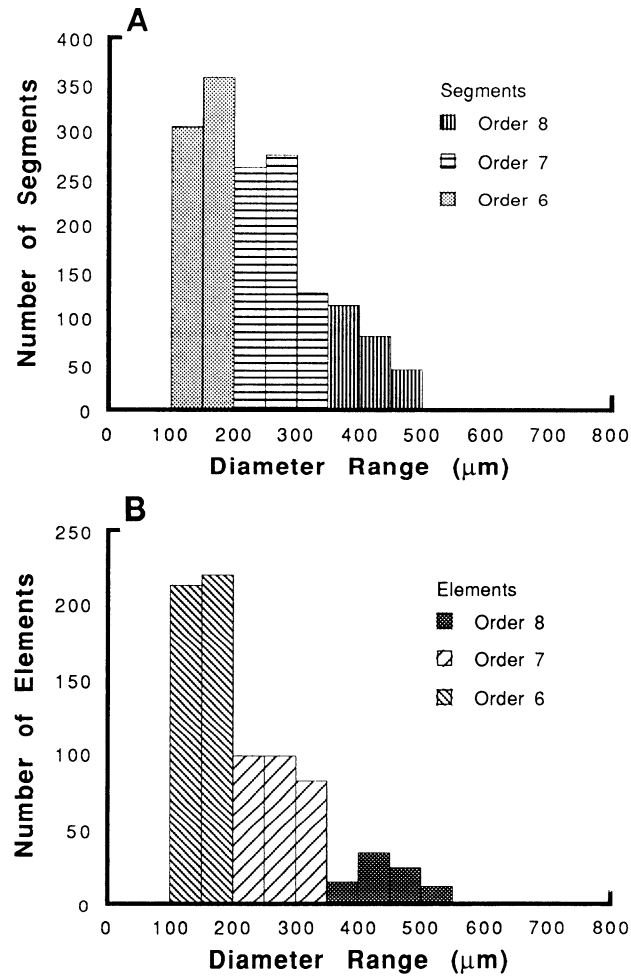

FIG. 7. Histograms of diameters of successive orders of vessels when order numbers are determined according to our "diameter-defined" method.

a very small fraction of the total population for *orders 1–3* but is a major fraction of the population for *orders 10* and *11*. The sample size affects the accuracy but not the quality of the histogram. If the values in each column (order) are divided by the sum total of that column, then we obtain the fraction of the number of elements of that specific order in specific intervals, and a plot of that fraction against the diameter gives a normalized histogram, which is an approximation of the probability frequency distribution of the diameters of the elements in each order. Table 5 shows the large overlap of the histograms of the successive orders of vessels when the order numbers were assigned in the conventional way.

Table 6 shows the number of elements in successive intervals of diameters in similar samples of the population of elements when the branching order numbers were assigned according to our "diameter-defined" method. In this method, a dividing line between the diameters of the vessels of successive orders is calculated from the means and standard deviations of the diameters according to *Eq. 3*. The dividing positions are detectable in the first column of Table 6 in the gaps between successive orders, e.g., 21–22, 38–39, and 53–54 μm. Between 1,101 and 1,550 μm there are no vessels. In the diameter-defined system, the probability frequency curves of successive orders have no overlap. Furthermore the histogram of

TABLE 5. *Distribution of diameters of elements in random samples in left pulmonary arterial trees*

Diam, μm	Order No.										
	1	*2*	*3*	*4*	*5*	*6*	*7*	*8*	*9*	*10*	*11*
1–10	39										
11–20	155	19									
21–30		52	5								
31–40		2	422	92							
41–50			58	330							
51–60			6	421	1						
61–70				332	103						
71–80				52	316						
81–90				4	268						
91–100					255	2					
101–150					183	197					
151–200						216					
201–250						59	40				
251–300						1	94				
301–350							77	4			
351–400							9	8			
401–450							6	27			
451–500							2	22			
501–550								14	3		
551–600								12	3		
601–650								1	1		
651–700								4	4		
701–750									5		
751–800									6		
801–850									0		
851–900									3	3	
901–950									3	5	
951–1,000										1	
1,001–1,050										3	
1,051–1,100										2	
1,101–1,150										1	
1,151–1,200										0	
1,201–1,250										0	
1,251–1,300										1	
1,301–1,550										0	0
1,551–1,600											2
1,601–1,650											0
1,651–1,700											2
1,701–1,750											0
1,751–1,800											0
1,801–1,850											1

Order nos. were determined according to conventional method of Strahler and Horsfield. Arterial trees are from 5 rats.

each order tends to be bell shaped when the intervals are small enough and sufficiently numerous.

DISCUSSION

Comparison With Other Work

Fung and Yen (2–4, 7) and Zhuang et al. (32) illustrated the usefulness of the type of data presented here in the pulmonary hemodynamics. Most existing morphometric data of the lung are based on Strahler's system. Singhal et al. (20) and Horsfield and Gordon (9, 12) presented data on the human pulmonary arterial and venous trees. Yen et al. (30, 31) presented data on the cat. Their order numbers were assigned according to Horsfield's rules (9). The following questions arise: When two vessels of the same order meet to generate one of similar size, should the order number be increased? When small branches emanate from a trunk along its length and the trunk appears tapered, should the order number be varied? In the existing system, there is no clear-cut rule. Yet decisions must have been made (9, 12, 20, 30, 31), although the exact rules were not stated. With *Eq. 3*, we offer a definite rule. Furthermore a clear distinction was made between segments and elements. We believe that, as a whole, their "branches" are in the nature of our "elements." Their data would have large overlaps of diameter ranges of the successive orders, as illustrated in Fig. 2 for rat data analyzed according to Horsfield's rule (9) (Table 5). These overlaps disappear in the diameter-defined Strahler system (Fig. 7), which is based on Table 6.

To describe the asymmetric bifurcation in a tree, Horsfield (10, 11) introduced a concept of "delta," which is the difference of the order numbers of two offshoots meeting at a bifurcation point. However, it is unlikely that delta is the same for all junctions of the blood vessels of a whole tree.

The lumping of segments of the same order connected in series into one element is an important step in the construction of analogue hemodynamic circuits, because vessels connected in series and in parallel differ tremendously in resistance. This is evident in an analogue electric circuit. Each segment is a resistor. If two resistors of resistance R each are connected in series, the total resis-

TABLE 6. *Distribution of diameters of elements in random samples in left pulmonary arterial trees*

Diam, μm	Order No.										
	1	*2*	*3*	*4*	*5*	*6*	*7*	*8*	*9*	*10*	*11*
1–10	32										
11–21	340										
22–30		102									
31–38		291									
39–53			782								
54–60				276							
61–72				465							
73–80					303						
81–90					304						
91–113					425						
114–150						211					
151–207						224					
208–250							79				
251–300							154				
301–337							45				
338–400								42			
401–450								47			
451–497								23			
498–550									14		
551–600									14		
601–650									10		
651–700									2		
701–745									0		
746–800										3	
801–850										2	
851–900										5	
901–950										4	
951–1,000										0	
1,001–1,050										7	
1,051–1,100										2	
1,101–1,291										0	
1,292–1,550											0
1,551–1,600											2
1,601–1,650											1
1,651–1,700											1
1,701–1,750											1

Order nos. were defined according to "diameter-defined" method. Arterial trees are from 5 rats.

tance is 2R. If they are connected in parallel, the total resistance is R/2. Hence, if several segments are connected in series into elements, they must not be mistaken as in parallel.

Qualitative and Quantitative Differences Between Diameter-Defined and Conventional Methods of Assigning Branching Order Numbers in Strahler's System

Statistical data of anatomy are used as a basis for constructing mathematical models for analysis. Let us examine the data against the observation that blood flows from larger to smaller arteries. In our silicone casts of pulmonary arteries, we have seen no exception to this rule. If we assumed that blood flows from arteries of *order n* to vessels of *order n* − 1, then the feature named above will not be preserved if the diameter histograms of successive orders of arteries have significant overlaps. For example, let all the histograms be normalized so that the total area is 1 in each case. If the diameter histogram of vessels of *order n* − 1 has a 10% overlap with that of *order n*, then there is a probability that in 10% of the smaller arteries of *order n* blood may flow into some larger arteries, which have a lower order number ($n - 1$). Inspection of the histogram data in Table 5 shows that, by following the conventional system of assigning order numbers, the overlaps of the diameter histograms of arteries of *orders 2–7* have overlaps as large as 20–40%. Hence, in modeling, considerable chaos would be permitted by the conventional method of ordering. On the other hand, with our diameter-defined ordering system, Table 6 shows that there is no overlap of histograms between successive orders, and the feature that blood flows from larger to smaller arteries has no chance of being violated.

Quantitatively, in constructing a mathematical model, one can assign any value to the diameter of an artery consistent with measured probability. Hence, the measured range of each variable is an important probability statement. Let us examine the ranges shown in Tables 5 and 6. For rat pulmonary artery of *order 4*, the diameter range specified by the conventional Strahler system is 31–90 mm (Table 5), whereas that specified by the diameter-defined system is 54–72 mm (Table 6). The range of conductance (the inverse of resistance), which is $(\pi/128\mu)D^4$, is 9.23–656.1 times $(\pi/128\mu) \times 10^5$ in the conventional system, whereas in the diameter-defined system, the conductance range is 85.0–268.7 times $(\pi/128\mu) \times 10^5$. In both cases, the statistical restrictions are much tighter when a model is constructed according to the diameter-defined system.

Handling of Tapered Vessels and Small Twigs

The advantage of the diameter-defined system becomes especially clear when one considers the ordering of long and tapered vessels, such as the main pulmonary arterial trunk shown in Fig. 3. Previous researchers were equivocal on such trunks. In our diameter-defined system, the long tapered trunk is divided into successive orders in a manner consistent with hemodynamics.

Hemodynamically, at a steady state, the rate of volume flow in a tapered tube is a constant at all cross sections, but the pressure gradient (dp/dx) varies along the longitudinal axis x. The Poiseuille formula is valid locally, and *Eq. 1* can be transformed to

$$\frac{dp}{dx} = \frac{128\mu\dot{Q}}{\pi}\frac{1}{D^4} \tag{7}$$

If the diameter of a linearly tapered tube is described by

$$D = D_0(1 - \alpha x) \tag{8}$$

where D_0 is the diameter at $x = 0$ and α is the taper rate, αD_0 is the axial rate of change of the diameter, dD/dx; then, on substituting *Eq. 8* into *Eq. 7* and integrating, we obtain the pressure drop at x in a tapered tube

$$p(x) - p_0 = \frac{128\mu\dot{Q}}{\pi D_0^4}\int_0^x \frac{1}{(1-\alpha x)^4}\,dx \tag{9}$$

where p_0 is the pressure at $x = 0$. When $\alpha \neq 0$, the pressure drop cannot be simulated by that in a straight tube, as in the conventional Strahler method, but it can be simulated by the pressure in a connected series of straight tubes with successively smaller diameters, which is the case in our diameter-defined system.

To a large extent the "small-twigs-off-the-large trunks" feature is accounted for by the connectivity matrix. Use of this matrix enables us to calculate the total number of elements in each order in a whole tree, even when the tree was pruned in the process of counting. The handling of pruned trees has always required a special explanation. The explanations of Refs. 9, 12, 20, 30, and 31 basically use a connectivity matrix. Thus our connectivity matrix formalizes a familiar thought and endows it with a quantitative expression.

Total Cross-Sectional Areas of Successive Orders of Arterial Elements Have Very Different Profiles for Rat, Human, and Cat

The total cross-sectional area of all elements of *order n*, designated A_n, can be calculated as the product of the area of each element and the total number of elements of *order n*. Thus

$$A_n = (\pi/4)D_n^2 N_n$$
$$\Delta A_n = (\pi/4)[(\Delta D_n^2) N_n + D_n^2 \Delta N_n] \tag{10}$$

If a simple analogue circuit is used in which all elements of *order n* are arranged in parallel, then the total pulmonary blood flow divided by A_n is the average velocity of the blood in the vessels of *order n*. At a steady state, the flow is constant for all n. Hence, the profile of A_n vs. n is the profile of the inverse of the blood velocity vs. the vessel order number n. The velocity divided by the vessel diameter is the shear strain rate, which is proportional to the shear stress that resists the blood flow. The rate of dissipation of energy is proportional to the product of shear stress and shear strain rate, i.e., to the velocity squared, or to the inverse of A_n^2.

The variation of A_n with the *order n* for the left lung of a rat is plotted in Fig. 8*A*. For the rat, A_n decreases with increasing n for n = 2–5, remains almost constant for n = 5–10, and then falls again for n = 11. For comparison, the data of Refs. 9, 20, and 31 are shown in Fig. 8, *B* and *C*. The human data from Horsfield (9) and Singhal et al. (20) show an exponential growth as the vessels become

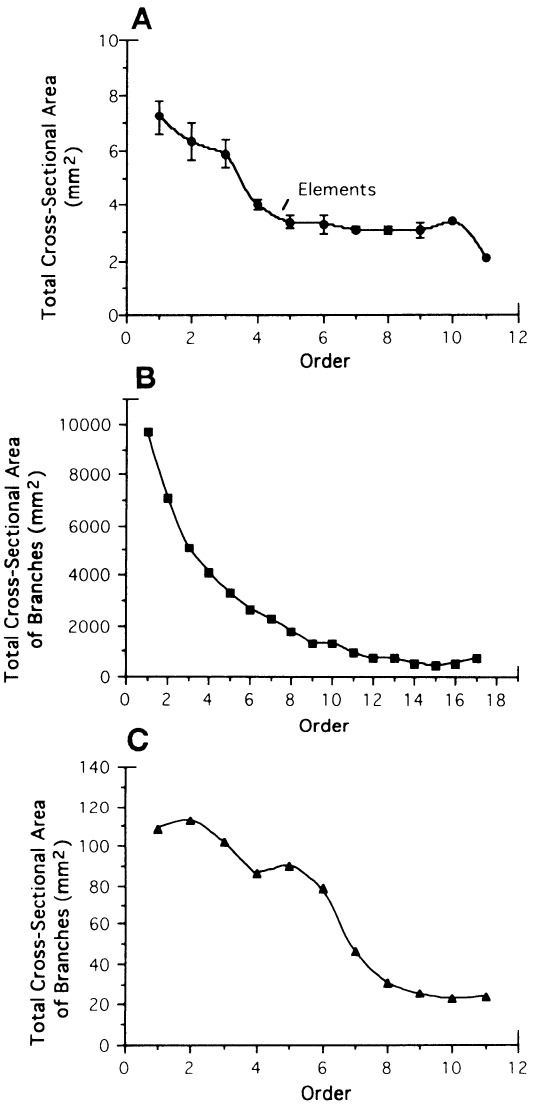

FIG. 8. Variation of total cross-sectional area of all parallel elements of each order with order number of elements. *A*: left lung of rat (our data). *B*: whole human lung (9). *C*: right lung of cat (31).

smaller, somewhat like the airways. The cat data from Yen et al. (31) show a trend closer to the data from the rat than from the human. The profiles of rat, cat, and human total arterial cross-sectional areas are very different from the profiles of their airways.

Applications of Flow Eqs. 1 and 2

Because the diameter, length, pressure, and flow are random variables in the statistical sense, in the application of *Eqs. 1* and *2* to a hemodynamic model, we need to assign values to D_m, L_m, P_n, and P_{m-1}, for $m = 1, 2, 3, \ldots, n \geq m$. For rat lung, the upper bound of m, n, is 11, and D_m and L_m are presented in Table 3. P_n refers to pressure in an arterial element of *order n* at the point of bifurcation where an element of *order m* takes off. P_n varies with the location of the bifurcation point and can be written as $P_n(x)$. If we say that the probability density of finding the bifurcation point at a point x along the vessel of *order n* is $f(x)$, then the expected value of $P_n(x)$ in *Eq. 2* is

$$P_n = \int_0^{L_n} P_n(x) f(x) dx \qquad (11)$$

This is the statistical average to be used in *Eqs. 1* and *2*. A similar treatment is required for P_{m-1}. If the probability of finding a branch from a vessel of *order n* at a point x is uniform along the vessel, then $f(x)$ is independent of x and P_n is just the spatial average of $P_n(x)$ along the vessel n.

An Alternate Statement of Some Morphometric Features

A major morphometric feature of the lung is a good order and regularity in the random variation of the diameters and lengths from one order to the next, as revealed in Figs. 5 and 6. In fact, the ratios of the diameters of successive orders are almost constant. This feature is said to be fractal according to a new mathematical terminology introduced by Mandelbrot (17, 18). Weibel (27) and West (28) argued that the language of fractals is uniquely suited for the analysis of the geometry and function of the lung. Mandelbrot classified fractals ac-

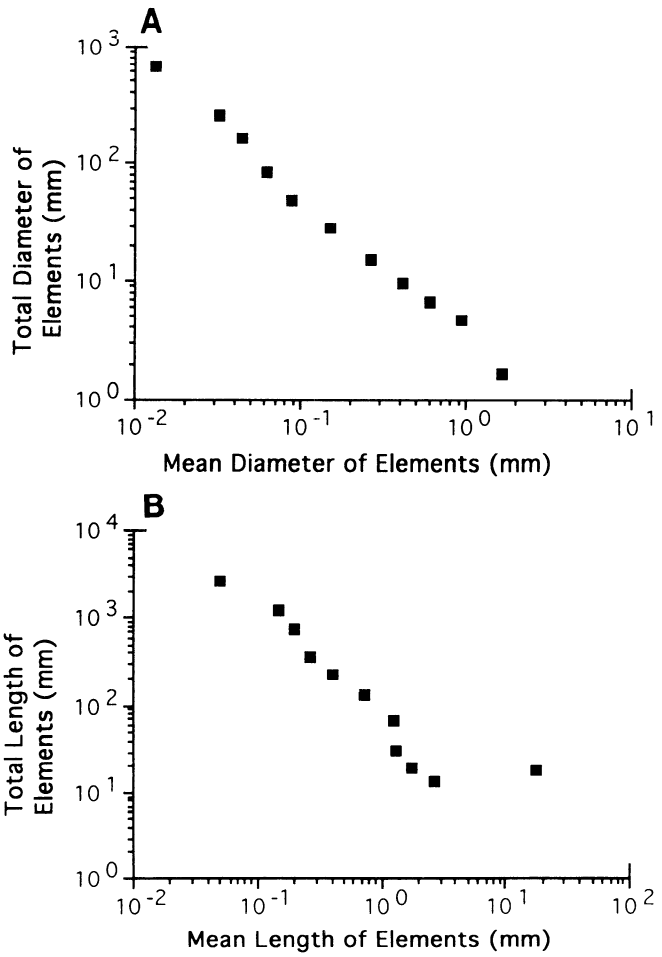

FIG. 9. Relationship between total length of a morphological feature (e.g., total length of elements, sum of diameters of elements) and basic length of measuring unit (e.g., length or diameter of a single element). Relationship is similar to that between total length of coastline of an island and length of measuring tape. Mathematical systems having such a behavior are said to be fractal. Each fractal system is characterized by slope of such a plot. From slope, a "fractal space dimension" can be computed (analogous to 1-, 2-, and 3-dimensional space). Each point represents specific order of arteries in left lung of rat.

cording to their dimensions. According to a formula given by Nelson (19)

$$1 - D_F = \log (\text{total size})/\log (\text{average size}) \quad (12)$$

we can compute the fractal dimension, D_F, and obtain $D_F = 2.15$ for the diameter and $D_F = 2.22$ for the length (Fig. 9) of the rat lung. Similarly, we can use the data of the pulmonary vessels of the human (9, 12) and the cat (30, 31) to determine the fractal dimensions for the diameter and the length. The results also lie between 2 and 3. These results show that the pulmonary arterial and venous trees possess the characteristics of fractal structure. However, the rat pulmonary system terminates in 11 orders, so the fractal feature is limited. Furthermore the connectivity matrix is not included in the conventional theory of fractals. The importance of the connectivity matrix should motivate a mathematical extension of the fractal theory to include such features.

This research was supported by National Heart, Lung, and Blood Institute Grants HL-43026 and HL-26647 and National Science Foundation Grant BCS-89-17576.

Address for reprint requests: Y. C. Fung, Institute for Biomedical Engineering, 0412, University of California, San Diego, 9500 Gilman Dr., La Jolla, CA 92093-0412.

Received 12 February 1993; accepted in final form 31 August 1993.

REFERENCES

1. **Cumming, G., R. Henderson, K. Horsfield, and S. S. Singhal.** The functional morphology of the pulmonary circulation. In: *The Pulmonary Circulation and Interstitial Space,* edited by A. Fisharan and H. Hecht. Chicago, IL: Univ. of Chicago Press, 1968, p. 327–338.
2. **Fung, Y. C.** *Biodynamics: Circulation.* New York: Springer-Verlag, 1984.
3. **Fung, Y. C.** *Biomechanics: Motion, Flow, Stress, and Growth.* New York: Springer-Verlag, 1990.
4. **Fung, Y. C.** Dynamics of blood flow and pressure-flow relationship. In: *The Lung: Scientific Foundations,* edited by R. G. Crystal, J. B. West, P. J. Barnes, N. S. Cherniack, and E. R. Weibel. New York: Raven, 1991, chapt. 5.2.2, p. 1121–1134.
5. **Fung, Y. C., and S. S. Sobin.** Elasticity of the pulmonary alveolar sheet. *Circ. Res.* 30: 440–450, 1972.
6. **Fung, Y. C., S. S. Sobin, H. Tremer, M. R. T. Yen, and H. H. Ho.** Patency and compliance of pulmonary veins when airway pressure exceeds blood pressure. *J. Appl. Physiol.* 54: 1538–1549, 1983.
7. **Fung, Y. C., and R. T. Yen.** A new theory of pulmonary blood flow in zone 2 condition. *J. Appl. Physiol.* 60: 1638–1650, 1986.
8. **Goldberger, A. L., and B. J. West.** Fractals in physiology and medicine. *Yale J. Biol. Med.* 60: 421–435, 1987.
9. **Horsfield, K.** Morphometery of the small pulmonary arteries in man. *Circ. Res.* 42: 593–597, 1978.
10. **Horsfield, K.** Diameters, generations, and orders of branches in the bronchial tree. *J. Appl. Physiol.* 68: 457–461, 1990.
11. **Horsfield, K.** Pulmonary airways and blood vessels considered as confluent trees. In: *The Lung: Scientific Foundations,* edited by R. G. Crystal, J. B. West, P. J. Barnes, N. S. Cherniack, and E. R. Weibel. New York: Raven, 1991, vol. I, p. 721–727.
12. **Horsfield, K., and W. I. Gordon.** Morphometry of pulmonary veins in man. *Lung* 159: 211–218, 1981.
13. **Horton, R. E.** Erosional development of streams and their drainage basins; hydrophysical approach to quantitative morphology. *Bull. Geol. Soc. Am.* 56: 275–370, 1945.
14. **Jiang, Z. L., and G. C. He.** Geometrical morphology of the human coronary arteries. *Acta Acad. Med. Mil. Tert.* 11: 85–91, 1989. (In Chinese with English abstract.)
15. **Jiang, Z. L., and G. C. He.** Geometrical morphology of coronary arteries in dog. *Chin. J. Anat.* 13: 236–241, 1990. (In Chinese with English abstract.)
16. **Kassab, G. S., C. A. Rider, N. J. Tang, and Y. C. Fung.** Morphometry of the pig coronary arterial trees. *Am. J. Physiol.* 266 (*Heart Circ. Physiol.* 35): H350–H365, 1993.
17. **Mandelbrot, B. B.** *Fractals: Form, Chance, and Dimension.* San Francisco, CA: Freeman, 1977.
18. **Mandelbrot, B. B.** *The Fractal Geometry of Nature.* San Francisco, CA: Freeman, 1982.
19. **Nelson, T. R.** Morphological modeling using fractal geometries. *Soc. Photo-Optical Instrum. Eng.* 914: 326–333, 1988.
20. **Singhal, S. R., R. Henderson, K. Horsfield, K. Harding, and G. Cumming.** Morphometry of the human pulmonary arterial tree. *Circ. Res.* 33: 190–197, 1973.
21. **Skalak, T. C., and G. W. Schmid-Schönbein.** The microvasculature in skeletal muscle. IV. A model of the capillary network. *Microvasc. Res.* 32: 333–347, 1986.
22. **Sobin, S. S., Y. C. Fung, H. M. Tremer, and T. H. Rosenquist.** Elasticity of the pulmonary alveolar microvascular sheet in the cat. *Circ. Res.* 30: 440–450, 1972.
23. **Sobin, S. S., H. M. Tremer, and Y. C. Fung.** Morphometric basis of the sheet-flow concept of the pulmonary alveolar microcirculation in the cat. *Circ. Res.* 26: 397–414, 1970.
24. **Strahler, A. N.** Quantitative analysis of watershed geomorphology. *Trans. Am. Geophys. Union* 38: 913–920, 1957.
25. **Weibel, E. R.** *Morphometry of the Human Lung.* Berlin: Springer-Verlag, 1963.
26. **Weibel, E. R.** Morphometric estimation of pulmonary diffusion capacity. I. Model and method. *Respir. Physiol.* 11: 54–75, 1970.
27. **Weibel, E. R.** Fractal geometry: a design principle for living organisms. *Am. J. Physiol.* 261 (*Lung Cell. Mol. Physiol.* 5): L361–L369, 1991.
28. **West, B. J.** Physiology in fractal dimensions. *Am. Sci.* 75: 354–365, 1987.
29. **Yen, R. T., Y. C. Fung, F. Y. Zhuang, and Y. J. Zeng.** Comparison of theory and experiments of blood flow in cat's lung. In: *Biomechanics in China, Japan, and USA.* Beijing, China: Science, 1984, p. 240–253.
30. **Yen, R. T., F. Y. Zhuang, Y. C. Fung, H. H. Ho, H. Tremer, and S. S. Sobin.** Morphometry of cat pulmonary venous tree. *J. Appl. Physiol.* 55: 236–242, 1983.
31. **Yen, R. T., F. Y. Zhuang, Y. C. Fung, H. H. Ho, H. Tremer, and S. S. Sobin.** Morphometry of cat's pulmonary arterial tree. *J. Biomech. Eng.* 106: 131–136, 1984.
32. **Zhuang, F. Y., Y. C. Fung, and R. T. Yen.** Analysis of blood flow in cat's lung with detailed anatomical and elasticity data. *J. Appl. Physiol.* 55: 1341–1348, 1983.
33. **Zhuang, F. Y., M. R. T. Yen, Y. C. Fung, and S. S. Sobin.** How many pulmonary alveoli are supplied by a single arteriole and drained by a single venule? *Microvasc. Res.* 29: 18–31, 1985.